Geophys. Astrophys. Fluid Dynamics, 1978, Vol. 10, pp. 25 52

Printed in Great Britain

Two-Layer Quasi-Geostrophic Turbulence in a Simple Special Case

RICK SALMON
Scripps Institution of Oceanography, La Jolla, California 92093, U.S.A.

(*Received May 31, 1977*)

In the case of equal layer depths and uniform vertical energy density, the quadratic integral invariants of two-layer rotating flow are close analogs of the corresponding invariants of two-dimensional turbulence. A simple theory based on the invariants and on the selection rules governing triad interactions qualitatively explains the major features of forced equilibrium flow. The general physical picture is very similar to that of Rhines (1977). In the geophysically interesting case, net baroclinic energy is produced at low wavenumbers and moves toward higher wavenumbers in relatively nonlocal triad interactions which are unhampered by the constraint to conserve enstrophy. The energy converts to barotropic mode and moves back toward low wavenumbers in more local interactions which are similar to those in two-dimensional turbulence. Equilibrium wavenumber spectra are obtainable from a simple Markovian turbulence closure model in which the estimate of turbulent scrambling rate includes a contribution from vortex stretching along the axis of rotation. Numerical experiments with the closure model confirm the qualitative predictions and demonstrate the sensitivity of the flow at low wavenumbers to changes in the forcing and dissipation.

1. INTRODUCTION

Stratified rotating flows would be a fascinating subject even if it were not that the earth's atmosphere and ocean are perhaps better characterized by these two adjectives than by any others. Such flows can store enormous quantities of potential energy in sloping density fields and convert the potential energy to kinetic energy in ways that tax human intuition. This paper modestly attempts to enlarge that intuition.

For simplicity, I focus on statistically homogeneous two-layer quasi-geostrophic flow in which the average energy density is invariant in the vertical direction. The flow is driven at low wavenumbers and damped by vertical-

boundary friction. My goal is to estimate the equilibrium wavenumber energy spectra and to explain the role of the various nonlinear interactions in shuttling the energy from the production wavenumbers to the dissipation wavenumbers.

Current understanding of stratified rotating dynamics comes from many sources. Two of importance are the theory of two-dimensional turbulence and baroclinic instability theory, which explains the short-term growth of larger-than-deformation-scale waves in the presence of an initially uniform baroclinic current. The instability problem was first solved by Charney (1947) and Eady (1949) and has since been re-solved with every conceivable refinement. Many of the refinements seem pointless indeed when one considers the enormity of the underlying approximation: infinitesimal energy in every wave. Recently Pedlosky (1970; 1972) has extended the instability calculation into the nonlinear regime, but his method is open to criticism in that turbulence is ruled out *a priori*.

The theory of two-dimensional turbulence began with Onsager (1949) and Fjortoft (1953) who independently deduced the single most distinctive property of two-dimensional flow—the transfer of energy from high to low wavenumbers—from simple conservation properties. In recent years the subject has been one of lively interest owing in large part to the development of new analytical tools which provide closed equations for the evolution of low-order flow statistics. The new tools have already found geophysical application in studies of atmospheric predictability (Leith, 1971; Leith and Kraichnan, 1972), two-dimensional flow on the β-plane (Holloway, 1977) and over topography (Herring, 1977; Holloway, 1977) and eddy viscosity (Kraichnan, 1976).

This paper extends the turbulence closure models to include stratification and thereby draws processes like baroclinic instability into the stochastic formulation. This is logical because baroclinic instability is in reality a triad interaction not fundamentally different from those of two-dimensional turbulence. The uniform point of view leads naturally to a simple picture of two-layer energy transfer which is disguised, I think, by the formal instability theory.

The restrictions to horizontally homogeneous flow and uniform vertical energy density are severe and probably destroy the possibility of useful direct comparison between my results and actual geophysical observations. Simple intuition dictates, after all, that coherent flow structures like jets and boundary currents are poorly characterized by their wavenumber spectra. Nonetheless, the present theory puts no unphysical restriction on the amount of energy in any spectral component or on the combinations of components which may interact with one another.

Section 2 presents a simple qualitative theory of two-layer flow based on the

quadratic integral invariants of the motion. The discussion is very similar to that of Rhines (1977), but here I emphasize the analogy between the two-layer dynamics and ordinary two- and three-dimensional turbulence. Section 3 describes the simple closure model which I have used to study two-layer turbulence. The development contains one new feature—the incorporation of vertical vortex stretching into the estimate of the turbulent scrambling rate—and may therefore be of some slight interest to those whose primary interest is turbulence theory. Section 4 presents the results of some experiments performed with the closure model. The paper is written in such a way that readers who have no interest in the details of the closure model may skip Section 3 without much loss in continuity.

2. QUALITATIVE THEORY

Consider a fluid system comprised of two immiscible layers of unequal density in uniform rotation about a vertical axis and confined between rigid horizontal plates. The governing quasigeostrophic equations of motion in the rotating reference frame are

$$\frac{\partial \zeta_i}{\partial t} + J(\psi_i, \zeta_i) = 0, \qquad i = 1, 2, \tag{2.1}$$

where ψ_1 is the streamfunction of the top layer, ψ_2 that of the bottom layer and

$$\zeta_i = \nabla^2 \psi_i + F_i(\psi_j - \psi_i), \qquad j = 3 - i. \tag{2.2}$$

The constants F_i are defined by $F_i = f^2/(g' D_i)$ where f is twice the rotation rate, D_i is the average depth of the ith layer, and g' the reduced gravity.

Equations (2.1–2.2) express the conservation of the potential vorticity ζ_i of each layer. These equations are usually derived from the general Navier-Stokes equations by an expansion in the Rossby number, which is assumed to be small. The Rossby number may be defined as the ratio ω/f where ω is the angular frequency that characterizes the motion of the fluid. A detailed derivation of (2.1–2.2) is given by Pedlosky (1970). Equation (2.1) may also be regarded as a vertical-finite-difference approximation to the more general quasi-geostrophic equation with continuous vertical density variation,

$$\frac{\partial \zeta}{\partial t} + J(\psi, \zeta) = 0, \tag{2.3a}$$

$$\zeta = \nabla^2 \psi + \frac{\partial}{\partial z}\left(\frac{f^2}{N^2(z)} \frac{\partial \psi}{\partial z}\right), \tag{2.3b}$$

where $N(z)$ = Vaisala frequency, in the case of isothermal ($\partial\psi/\partial z$ = constant)

vertical boundary conditions. Except for their neglect of horizontal variations in f and D_2, both (2.1) and (2.3) are respectable model equations for the geophysical fluids.

In this paper, I restrict attention to solutions of (2.1) with $D_1 = D_2$ in which the upper and lower layers have identical horizontal wavenumber energy spectra. These combined assumptions will be referred to as the special case of "equivalent layers". The assumption of equivalent layers is a severe restriction, but it greatly simplifies the analysis in Section 4. Figure 1 shows a schematic model which corresponds to the equivalent layers case. The propellers, which represent mechanical energy sources, may be correlated or uncorrelated, but they turn always with the same average power. The vertical boundaries have identical drag coefficients.

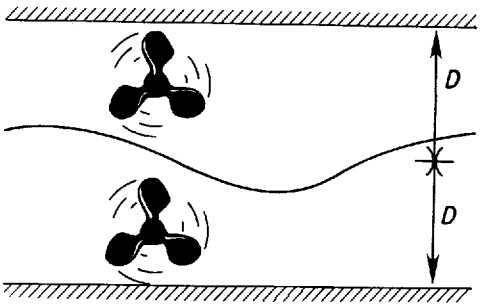

FIGURE 1 Schematic drawing of a system with equivalent layers.

Because of the equivalent layers, it is convenient to recast (2.1) in terms of vertical modal streamfunctions. Let $\psi + \tau$ be the upper streamfunction and $\psi - \tau$ the lower. Then (2.1) converts to

$$\nabla^2\psi_t + J(\psi, \nabla^2\psi) + J(\tau, \nabla^2\tau) = S_\psi, \tag{2.4a}$$

and

$$\nabla^2\tau_t + J(\psi, \nabla^2\tau) + J(\tau, \nabla^2\psi) - S_\tau = k_R^2[\tau_t + J(\psi, \tau) - H], \tag{2.4b}$$

where $k_R^{-1} = (2F)^{-1/2}$ is the internal Rossby radius of deformation. The deformation radius is about 40 km in the mid-latitude ocean and about ten times larger in the atmosphere. Equation (2.4b) may be interpreted as either a baroclinic vorticity equation in which the right side represents the vorticity production by vertical vortex stretching, or as a temperature equation in which the left side is proportional to the vertical advection of temperature. The symbols S_ψ, S_τ and H represent hypothetical stirring and heating forces. Heating is understood to mean the transfer of fluid mass between the layers.

Baroclinic stirring and heating are dynamically equivalent because the quasi-geostrophic equations enforce the thermal wind relation.

As in the case of homogeneous turbulence, important energy transfer properties of (2.4) may be deduced from the quadratic integral invariants of the motion. Under adiabatic conditions (2.4) conserves total mechanical energy, and the potential enstrophy,

$$\tfrac{1}{2}\iint (\zeta_i^2)dx\ dy,$$

of each layer. Under the assumption of equivalent layers, the enstrophies are identical and the three invariants degenerate to two. In this circumstance, the two layer dynamics has an illuminating analogy with ordinary homogeneous turbulence.

Let the streamfunctions be expanded in Fourier series in the usual way:

$$\psi = \sum_{\mathbf{k}} \psi_{\mathbf{k}} \exp[i\mathbf{k}\cdot\mathbf{x}], \qquad \tau = \sum_{\mathbf{k}} \tau_{\mathbf{k}} \exp[i\mathbf{k}\cdot\mathbf{x}].$$

Then the constraints become

$$\frac{d}{dt}\sum_{\mathbf{k}} [\mathrm{U}(\mathbf{k}) + \mathrm{E}(\mathbf{k})] = 0, \tag{2.5a}$$

and

$$\frac{d}{dt}\sum_{\mathbf{k}} [k^2 \mathrm{U}(\mathbf{k}) + (k^2 + k_R^2)\,\mathrm{E}(\mathbf{k})] = 0, \tag{2.5b}$$

where $\mathrm{U}(\mathbf{k}) \equiv k^2 \langle|\psi_{\mathbf{k}}|^2\rangle$ and $\mathrm{T}(\mathbf{k}) \equiv k^2 \langle|\tau_{\mathbf{k}}|^2\rangle$ are proportional to the barotropic and baroclinic kinetic energies in wavenumber $\mathbf{k}$ and

$$\mathrm{E}(\mathbf{k}) = (1 + k_R^2/k^2)\,\mathrm{T}(\mathbf{k})$$

is the *total* baroclinic energy. The symbol $\langle\ \rangle$ denotes ensemble average, which of course is optional in (2.5). The difference between $\mathrm{E}(\mathbf{k})$ and $\mathrm{T}(\mathbf{k})$ is the available potential energy.

Equations (2.5a, b) constitute the first law of thermodynamics for the spectrally truncated version of (2.4). The corresponding second law of thermodynamics is

$$\frac{d}{dt_I}\sum_{\alpha} [\log \mathrm{U}_\alpha + \log \mathrm{E}_\alpha] \geqq 0, \tag{2.6}$$

where d/dt_I refers to the tendency arising from interactions between the spectral components and α is an index which specifies both $\mathbf{k}$ and real or imaginary part of $\psi_{\mathbf{k}}$ and $\tau_{\mathbf{k}}$. Equation (2.6) is simply derived by the methods of information theory with the individual spectral intensities U_α and E_α regarded as "information". The derivation hinges on the fact that Liouville's theorem holds in the phase space spanned by the ψ_α, τ_α. Under adiabatic conditions, the absolute equilibrium state is discovered by maximizing the sum in (2.6) subject to (2.5). The result, which is identical to that given by Salmon *et al.* (1976), has

$$E(k)=U(\{k^2+k_R^2\}^{1/2}).$$

and the maximum entropy spectra are thus extremely deficient in large scale baroclinic energy in cases of geophysical interest.

The importance of (2.5) lies not so much in its implications for absolute equilibrium (which is never approached in real fluids) as in the fact that individual triad interactions are subject to the same constraints. Perusal of (2.4) indicates two types of triad in the two layer fluid. One type consists of three barotropic components and the other consists of one barotropic and two baroclinic components. Let $\mathbf{k}, \mathbf{p}, \mathbf{q}$ be any three wavenumbers that sum to zero. The energy transfer in the two types of triad is then constrained by

$$\dot{U}(\mathbf{k})+\dot{U}(\mathbf{p})+\dot{U}(\mathbf{q})=0, \tag{2.7a}$$

$$k^2\ \dot{U}(\mathbf{k})+p^2\ \dot{U}(\mathbf{p})+q^2\ \dot{U}(\mathbf{q})=0, \tag{2.7b}$$

and

$$\dot{U}(\mathbf{k})+\dot{E}(\mathbf{p})+\dot{E}(\mathbf{q})=0, \tag{2.8a}$$

$$k^2\ \dot{U}(\mathbf{k})+(p^2+k_R^2)\ \dot{E}(\mathbf{p})+(q^2+k_R^2)\ \dot{E}(\mathbf{q})=0, \tag{2.8b}$$

where the tendencies are those resulting from interaction with other members in the triad.

The constraints (2.7a, b) are the same as for ordinary two-dimensional turbulence. In (2.7) suppose $k \leqq p \leqq q$. As is well known, (2.7b) prevents effective energy transfer between different scales of motion in both extremely local ($k \approx p$) and extremely nonlocal ($k \ll p$) triads. For intermediate k, p, q the spreading of energy from middle to outer wavenumbers generally favors the lower wavenumber; this is the familiar "leftward" energy transfer. In three-dimensional turbulence, only (2.7a) holds, and any shape triad may transfer energy between scales. In three dimensions there is no inhibition against rightward energy transfer.

For the baroclinic triads, k_R represents a physically important dividing scale. When $k, p, q \gg k_R$ the constraints (2.8) are the same as (2.7) so that energy

transfer in the baroclinic triads is the same as in two-dimensional turbulence. This agrees with the physical picture of two-layer flow on scales smaller than the deformation radius as being essentially uncoupled single layers in which vortex stretching is insignificant. However, (2.8b) shows that the situation with $k, p, q \ll k_R$ is much more akin to three-dimensional turbulence. In this case, the energy transfer is between the two baroclinic components only and may be either local ($p = 0(q)$) or nonlocal ($p \ll q$). Because of k_R^2 in (2.8b), the enstrophy constraint poses no inhibition to the rightward transfer of baroclinic energy on $k < k_R$. If $k = 0(k_R)$ in (2.8) then energy is passed to the barotropic component $\mathbf{U}(\mathbf{k})$ as well.

A much studied class of UEE triads are the "baroclinic instability" triads ($k \approx q \gg p \to 0$), in which the initial energy resides wholly in p. Isosceles interactions of this kind are the only ones possible for a short time after the onset of decay of a horizontally uniform baroclinic current. However, as the higher wavenumbers populate with energy, more general interactions satisfying (2.8) become possible and the isosceles interactions lose their special status.

Simple arguments such as those given above may be used to intuit the general movement of energy in the two-layer system. Consider a hypothetical two-layer fluid with a minimum wavenumber $k_0 \ll k_R$ near which stirring and/or heating forces act. Dissipation is also present, but, for simplicity, it is constrained to act in only two regions of the spectrum: near k_0, where it models the loss of large scale energy to Ekman-type vertical boundary layers, and near $k_D \gg k_R$, where it parameterizes the transition from two- to three-dimensional flow on scales too small to feel the rotation. In the general inertial region, $k_0 < k < k_D$, neither forcing nor dissipation is significant.

Under steady forcing conditions, the fluid is assumed to reach a statistically steady state in which the transfer of total energy and potential enstrophy past k is the same for every k in $k_0 < k < k_D$. Now, on scales smaller than the deformation radius, the dynamics are those of uncoupled but statistically identical single layers in which the general invariants reduce to ordinary kinetic energy and enstrophy. Since the only energy sources are at k_0, we may expect k^{-3} enstrophy-cascading inertial ranges on $k_R < k < k_D$. If k_D/k_R is large, then the energy reaching k_D is negligible. This means that the large scales must adjust to a state in which the net energy production at k_0 is zero, that is

$$\dot{\mathcal{U}}(k_0)_{nc} = -\dot{\mathcal{E}}(k_0)_{nc},$$

where $\mathcal{U}$ and $\mathcal{E}$ are the angularly-integrated spectra defined by

$$\int_0^\infty \mathcal{U}(k)dk = 2 \sum_{\mathbf{k}} \mathbf{U}(\mathbf{k}),$$

and

$$\int_0^\infty \mathscr{E}(k)dk = 2\sum_{\mathbf{k}} \mathrm{E}(\mathbf{k}),$$

and the subscripts *nc* denote tendencies due to forcing and dissipation. The potential enstrophy production,

$$k_R^2\, \dot{\mathscr{E}}(k_0)_{nc}dk,$$

equals the transfer rate of potential enstrophy across $k_0 < k < k_D$, and it must be positive because there is only an enstrophy sink at k_D. Now since $\dot{\mathscr{E}}(k_0)_{nc} > 0$ while $\dot{\mathscr{U}}(k_0)_{nc} < 0$, internal interactions must act to transfer large scale energy from baroclinic to barotropic mode. However, by the reasoning given above, large scale baroclinic components may transfer energy only between themselves. The transfer from baroclinic to barotropic mode must therefore occur on $k_0 < k < k_R$ as a rightward transfer of baroclinic energy in UEE triads and an equal and opposite leftward transfer of barotropic energy in UUU triads. The conversion of baroclinic to barotropic energy can occur near k_R. The above arguments are *not* strongly dependent upon the equivalent layers assumption, and, in fact, all of the preceding equations continue to hold if this assumption is relaxed.

Figure 2, which is very similar to a figure of Rhines (1977), is a schematic wavenumber energy flow diagram for the hypothetical two-layer system discussed above. Potential enstrophy transfer, which may be deduced by similar arguments, is indicated by dashed arrows on the same diagram. Figure 2 is suggestive of, but different from the wavenumber energy flow diagrams conventionally drawn in meteorology. In Figure 2, for example, *both* the upper horizontal and the vertical arrows represent a conversion of potential to kinetic energy.

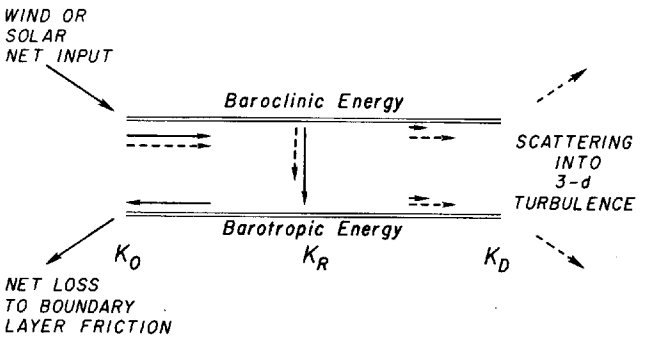

FIGURE 2 The wavenumber energy flow diagram for a two-layer system. The solid arrows represent energy flow, and the dashed arrows, potential enstrophy flow.

Rhines (1977) has studied the free evolution of two-layer turbulence from random initial conditions in extensive numerical experiments. He finds that large scale baroclinic currents decay rapidly to deformation scale eddies which quickly become barotropic and then gradually increase their scale in the sequence suggested by Figure 2.

Nonlocal triad interactions are probably responsible for the quickness of the rightward energy transfer in Rhines' experiments. One is tempted to draw an analogy between this process and the rapid initial energy transfer from low to high wavenumbers in ordinary three-dimensional turbulence when the energy is initially concentrated at the low wavenumbers. The latter process corresponds in physical space to the stretching of thin vortex tubes by the large-scale shear. The classical baroclinic instability problem offers a corresponding but less simple physical space picture of nonlocal energy transfer in the two-layer system. Let $\tau = Vy$ locally in physical space with V a constant shear velocity and infinitesimal initial energy in the higher wavenumbers. Then the waves with $k < k_R$ are unstable and the fastest growing have wavevectors pointing in the x-direction. An elementary and well known stability analysis gives

$$\mathrm{U}(\mathbf{k}, t) = \mathrm{U}(\mathbf{k}, 0) \exp\left\{2Vk\sqrt{\frac{k_R^2 - k^2}{k_R^2 + k^2}}\, t\right\}, \tag{2.9a}$$

and

$$\mathrm{E}(\mathbf{k}, t) = (k_R^2/k^2 - 1)\ \mathrm{U}(\mathbf{k}, t), \tag{2.9b}$$

for the energy in growing x-directed waves. It can easily be checked that (2.9) is consistent with (2.8).

In this paper I am chiefly concerned with two-layer fluids which are in equilibrium with a statistically steady forcing and damping. For such systems, the degree of nonlocalness of the baroclinic interactions comprising the rightward energy transfer is of interest. Intuition based on the hydrodynamical stability calculation suggests that a major part of this transfer may occur in extremely nonlocal triads that link k_0 directly with k_R. However, this conclusion may not hold for fully developed turbulence in which the distorting influence of intervening scales becomes important.

A more quantitative analysis of two-layer turbulence requires numerical methods. Direct simulation of the equations of motion would naturally be the most desirable attack. Unfortunately, the computations required to first step the system to equilibrium and then average long enough to obtain accurate statistics make such an approach uneconomical if not actually impossible. A class of turbulence closure models reviewed by Orszag (1970) offers an attractive alternative. The closure models predict the evolution of wavenumber spectra from the spectra themselves. The closure equations are nonlinear,

but they can be solved more efficiently than the equations of motion for reasons connected with the smoothness of statistics versus the jumpiness of individual realizations. The next section describes the simple closure model I have used to study the equivalent layers case.

3. QUANTITATIVE THEORY

Suppose now that the turbulence is horizontally homogeneous and isotropic. It follows directly from (2.4) that

$$\dot{\mathrm{U}}(k)=2\sum_{\mathbf{p}+\mathbf{q}=\mathbf{k}}(\mathbf{p}\times\mathbf{k})q^2\ \mathrm{Re}\{\langle\psi_{\mathbf{p}}\psi_{\mathbf{q}}\psi_{-\mathbf{k}}\rangle+\langle\tau_{\mathbf{p}}\tau_{\mathbf{q}}\psi_{-\mathbf{k}}\rangle\}, \tag{3.1a}$$

and

$$\dot{\mathrm{E}}(k)=2\sum_{\mathbf{p}+\mathbf{q}=\mathbf{k}}(\mathbf{p}\times\mathbf{k})(q^2-p^2+k_R^2)\ \mathrm{Re}\langle\psi_{\mathbf{p}}\tau_{\mathbf{q}}\tau_{-\mathbf{k}}\rangle, \tag{3.1b}$$

where $\mathbf{p}\times\mathbf{k}=p_xk_y-p_yk_x$ and Re denotes the real part. Equations (3.1) are the first in a hierarchy of statistical moment equations which are exact but unusable unless a closure approximation is invoked to reduce the number of dependent variables. Here I use the eddy-damped Markovian (EDM) approximation proposed by Orszag (1970; 1974) for homogeneous turbulence. The deduction of *two-layer* EDM equations differs in no essential respect from Orszag's derivation, and therefore only the final result will be given. Readers who are interested in the somewhat lengthy details should consult the papers by Orszag, or Leith (1971). The EDM approximation to (3.1) is as follows:

$$\dot{\mathcal{U}}(k)=\iint^{\Delta}dp\,dq\,\{\mathrm{T}(k,p,q)+S(k,p,q)\}+F_{\mathrm{U}}(k), \tag{3.2a}$$

$$\dot{\mathcal{E}}(k)=\iint^{\Delta}dp\,dq\,\{M(k,p,q)\}+F_{\mathrm{E}}(k), \tag{3.2b}$$

$$\mathrm{T}(k,p,q)=4\pi k\,D_1(k,p,q)\,B_1(k,p,q)[\mathrm{U}(p)\,\mathrm{U}(q)-\mathrm{U}(q)\,\mathrm{U}(k)], \tag{3.3a}$$

$$S(k,p,q)=4\pi k\,D_2(k,p,q)\,B_2(k,p,q)[\mathrm{E}(p)\,\mathrm{E}(q)-\mathrm{E}(q)\,\mathrm{U}(k)], \tag{3.3b}$$

$$M(k,p,q)=4\pi k\,D_2(p,k,q)\,\{B_3(k,p,q)\,\mathrm{U}(p)\,\mathrm{E}(k)+B_4(k,p,q)\,\mathrm{E}(q)\,\mathrm{E}(k)+B_5(k,p,q)\,\mathrm{U}(p)\,\mathrm{E}(q)\}, \tag{3.3c}$$

$$\frac{d}{dt}D_1(k,p,q)=1-\{\mu_\psi(k)+\mu_\psi(p)+\mu_\psi(q)\}\,D_1(k,p,q), \tag{3.4a}$$

$$\frac{d}{dt}D_2(k,p,q)=1-\{\mu_\psi(k)+\mu_\tau(p)+\mu_\tau(q)\}\,D_2(k,p,q), \tag{3.4b}$$

$$D_i(k,p,q)=0\quad\text{at}\quad t=0,\qquad i=1,2. \tag{3.5}$$

In the above equations, $U(k)$ and $E(k)$ are understood to mean what were previously $U(\mathbf{k})/d\mathbf{k}$ and $E(\mathbf{k})/d\mathbf{k}$. The wavenumber integration in (3.2) extends over that part of the positive p–q quadrant for which line segments of lengths k, p, q can form triangles. $F_U(k)$ and $F_E(k)$ are hypothetical spectral forcing functions, and the $B_i(k, p, q)$ are time-invariant "geometrical coefficients" which are given explicitly in the appendix.

The quantities $D_1(k, p, q)$ and $D_2(k, p, q)$, which have the dimensions of time, are physically interpretable as average persistence times for the triple products $\psi_p\psi_q\psi_{-k}$ and $\tau_p\tau_q\psi_{-k}$ respectively. The initial condition (3.5) corresponds to random initial specification of ψ_k and τ_k for given initial spectra. The $\mu_\psi(k)$ and $\mu_\tau(k)$ are intrinsic auto-decorrelation rates for the factors ψ_k and τ_k in these same triple products. That is, $\mu_\psi(k)$ and $\mu_\tau(k)$ measure the rate at which turbulent scrambling of ψ_k and τ_k by all other wavenumbers erodes the triple correlations responsible for spectral energy transfer in (3.1). Equations (3.2–3.5) are of course not truly closed until $\mu_\psi(k)$ and $\mu_\tau(k)$ are specified, and the EDM formalism offers no unique way to do this.

Equations (3.2–3.5) are exact for short times after random initial conditions. For any positive choice of $\mu_\psi(k)$ and $\mu_\tau(k)$ the equations maintain the proper quadratic integral invariants of the motion, and under adiabatic conditions they tend asymptotically to the correct absolute equilibrium states. In writing (3.2–3.5) I have made repeated use of the equivalent layers assumption. If the assumption is relaxed, then terms containing $\langle\psi_k\tau_{-k}\rangle$ appear in (3.2) and an evolution equation for this quantity must be developed. The equivalent layers assumption is thus a diagonalizing approximation which is analogous to vertical statistical homogeneity for (2.3).

The EDM equations are the simplest in a class of models all of which have energy equations similar to (3.2). The models differ primarily in the way they specify the $\mu(k)$ or their appropriate generalization. Kraichnan's (1959) direct interaction approximation (DIA) is usually considered to be the most fundamental model because the others can be looked on as abridgments of DIA. Both the DIA and its Lagrangian-history extension (Kraichnan, 1965) are examples of fully self-consistent models which contain no adjustable parameters or unspecified quantities.

Unfortunately, the fully self-consistent models are somewhat more complex than (3.2–3.5) and their solution requires a substantial computing effort. A practical alternative, which has been followed by several investigators, is to retain the relatively simple form of equations like (3.2–3.5) and to specify the $\mu(k)$ by heuristic physical or even dimensional arguments. Although this is distasteful from a theoretical point of view, numerical tests of such theories have been very encouraging. For example, Herring *et al.* (1974) have shown that the predictions of the test field model (Kraichnan, 1971a) agree well with direct simulations of the equations of motion for two-dimensional turbulence

at moderate Reynolds number. At very large Reynolds number, the test field model is at least consistent with the predictions of inertial range theories.

In this paper, I prescribe the $\mu(k)$ by simple arguments which may be considered an extension of a formula proposed by Pouquet *et al.* (1975) for two-dimensional turbulence. With $k_R = 0$, the two-layer equations degenerate to those for uncoupled single layers for which Pouquet suggests the closure†

$$\mu(k) = \mu_\tau(k) = \mu_H(k), \tag{3.6}$$

where

$$\mu_H(k) \equiv \lambda_H \left\{ \tfrac{1}{2} \int_0^k p^2 [\mathcal{U}(p) + \mathcal{T}(p)] dp \right\}^{1/2}, \tag{3.7}$$

$$\mathcal{T}(p) = p^2 \, \mathcal{E}(p)/(p^2 + k_R^2),$$

is the baroclinic *kinetic* energy spectrum, and λ_H is an order one constant. The quantity $\mu_H^{-1}(k)$ is a logical kinematic estimate of the time required for an eddy of scale k^{-1} to undergo a significant distortion. For $\mathcal{U}(p)$ and $\mathcal{T}(p)$ rapidly decreasing with p, (3.7) agrees asymptotically with the corresponding expression in the test field model if

$$\lambda_H = 0.434 \; g, \tag{3.8}$$

where g is the adjustable parameter in the test field model. It can be shown (Kraichnan, 1971b; Pouquet *et al.*, 1975) that (3.2–3.7) with $k_R = 0$ admits both $k^{-5/3}$ and (log-corrected) k^{-3} inertial range solutions and that the predicted values of Kolmogorov's constant are proportional to $\lambda_H^{2/3}$ in either range.

In the general case $k_R \neq 0$ the layers are coupled and the nonlinear terms of the right side of (2.4b) constitute an additional source of turbulent scrambling for τ. Physically speaking, distortions in the streamfunction field now arise from *both* the horizontal vorticity advection and the vertical vortex stretching. The latter effect enhances $\mu_\tau(k)$ for $k < k_R$, but $\mu_\psi(k)$ could be nearly unchanged since no stretching terms appear in (2.4a).

To see the physics more clearly, consider not (2.4) but its antecedent (2.3) and assume for convenience that $N(z)$ is a constant. Then the expression (2.3b) for the potential vorticity ζ is invariant to permutations in x, y and the stretched coordinate Nz/f. From this fact Charney (1971) argued that stratified quasi-geostrophic turbulence ought to be fully isotropic in $(x, y, Nz/f)$ on horizontal scales L for which fL/N is small compared to the depth of the fluid. For flow confined between horizontal planes (Fig. 3) the larger scales of

†My notation.

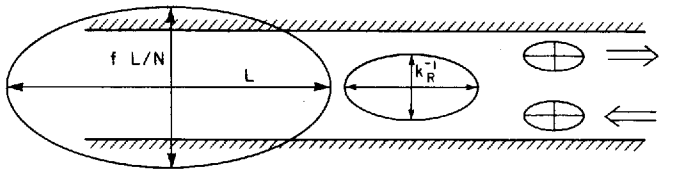

FIGURE 3 Eddies of potential vorticity confined between parallel plates.

motion cannot have this property, but fL/N still defines the vertical scale over which potential vorticity eddies of horizontal scale L are sensitive to changes in the flow. The internal radius of deformation separates the large eddies whose vertical range extends through the full depth of the fluid from the smaller eddies whose vertical range is small.

Now if shear is present in only the gravest vertical mode as suggested by the arrows on the right of Figure 3, then the shear distorts only the eddies of horizontal scale larger than the deformation radius. Smaller eddies are displaced relative to one another by the shear, but this displacement is dynamically unimportant since there is no significant vertical coupling on these scales. The rate of strain caused by the vertical shear is a plausible estimate of the scrambling rate due to the vertical coupling terms and I therefore complete (3.2–3.5) with

$$\mu_\psi(k)=\mu_H(k), \tag{3.9a}$$

and

$$\mu_\tau(k)=\{\mu_H^2(k)+\mu_v^2(k)\}^{1/2}, \tag{3.9b}$$

where $\mu_H(k)$ is given by (3.7) and measures the scrambling effect of the horizontal shear, and

$$\mu_v(k)=\lambda_v \exp\{-k^2/k_R^2\}kv_{rms} \tag{3.10}$$

measures the effect of vertical shear. In (3.10) λ_v is order one and

$$v_{rms}=\left\{\tfrac{1}{2}\int_0^k \mathscr{T}(p)dp\right\}^{1/2} \tag{3.11}$$

is the *rms* velocity of one layer relative to the other (excluding scales smaller than k^{-1}). Thus for $k<k_R$, $\mu_v^{-1}(k)$ is the advective dephasing time of an eddy of size k^{-1} by the vertical shear.

The physical ideas underlying (3.9–3.11) are heuristic and it would be pointless to defend them very strongly. The most convincing proof of their

utility is the rather good agreement between solutions of (3.2–3.5 and 3.7–3.11) and (2.4) described below. It is interesting, however, to contrast the predictions of the closure theory with (2.9) for the case of an initially uniform baroclinic current. Putting

$$E(p)=\frac{k_R^2\,V^2}{p^2}\,\delta(\mathbf{p}-\mathbf{p}_0) \tag{3.12}$$

in the general EDM equations for anisotropic flow and passing carefully to the limit $\mathbf{p}_0\to\infty$ one obtains the following expressions for the energy in the most unstable mode with scalar wavenumber k.

$$U(\mathbf{k},t)=U(\mathbf{k},0)\exp\left\{4k^2\,D_2(k,k,0)\frac{(k_R^2-k^2)}{(k_R^2+k^2)}\,V^2t\right\}, \tag{3.13a}$$

$$E(\mathbf{k},t)=\left(\frac{k_R^2}{k^2}-1\right)U(\mathbf{k},t). \tag{3.13b}$$

After times longer than $\mu_\tau^{-1}(k)$, (3.4) has

$$D_2(k,k,0)\approx\mu_\tau^{-1}(k), \tag{3.14}$$

so that (3.13–3.14) agrees with (2.9) if

$$\mu_\tau(k)=2kV(k_R^2-k^2)^{1/2}\,(k_R^2+k^2)^{-1/2}. \tag{3.15}$$

But if $\lambda_v=2$, (3.15) agrees with (3.9–3.11) up to order k^2/k_R^2 for the unstable modes with $k<k_R$. Thus $\lambda_v=2$ constitutes the best fit to the instability problem.

To test the closure theory against fully developed turbulence, I compare direct simulations of (2.4) with solutions of (3.2–3.5 and 3.7–3.11) for various values of λ_v. In all cases $\lambda_H=0.282$, which corresponds to $g=0.65$ in (3.8). Herring *et al.* (1974) have shown that the test field model compares well with two-dimensional turbulence simulations for a value of g in this range. Equations (2.4) were solved by the algorithm invented by Orszag (1971) with no aliasing. The primary arithmetical task in the solution of the closure equations is the evaluation of the wavenumber integrals in (3.2). Dr. J. R. Herring very kindly loaned me a complete computer package for evaluating integrals of this type. For both sets of equations the wavenumbers run from $k_{\min}=1$ to $k_{\max}=32$ with $k_R=15$. Such choice drastically under-represents the

sub-deformation scales for which, however, considerable confidence in the closure theory already exists. Forcing and damping are introduced in (2.4) via

$$\begin{matrix}(a) & (b)\\ S_\psi = -\lambda\nabla^2\psi & -\alpha(k)\nabla^2\psi,\end{matrix} \tag{3.16a}$$

$$\begin{matrix}(a) & (b) & (c)\\ S_\tau = -\lambda\nabla^2\tau & -\alpha(k)\nabla^2\tau + J,\end{matrix} \tag{3.16b}$$

$$\begin{matrix}(d) & (b)\\ H = -\lambda'\tau & -\alpha(k)\tau,\end{matrix} \tag{3.16}$$

where the terms designated by letters represent:

(a) Ekman layer drag (on both vertical boundaries);
(b) the removal of energy from $k < k_{max}$ by interactions involving higher wavenumbers;
(c) baroclinic stirring (or heating); and
(d) Newtonian heat transfer between the layers.

The eddy viscosity (b) is required to prevent enstrophy from piling up spuriously near k_{max}. In the experiments described below $\lambda = \lambda'$ and, following Holloway (1976),

$$\alpha(k) = \begin{cases} 0 \quad , & k < k_e, \\ \nu_0 \, k_{max}^2 \, \dfrac{(k^2 - k_e^2)^2}{(k_{max}^2 - k_e^2)^2} \, , & k > k_e, \end{cases} \tag{3.17}$$

with $k_e = 15$ in the experiments of this section. The constant ν_0 is chosen more or less arbitrarily to give the spectra a smooth appearance near k_{max}. In this section $\nu_0 = 0.002$. Equations (3.16) correspond to

$$F_U(k) = -2(\lambda + \alpha(k))\mathscr{U}(k), \tag{3.18a}$$

and

$$F_E(k) = -2(\lambda + \alpha(k))\,\mathscr{E}(k) + J(k), \tag{3.18b}$$

in (3.2). With friction included, the quantity $\lambda + \alpha(k)$ is added to the right sides of (3.9). For the forcing term J, I literally used a negative drag coefficient on $k < 3.5$. Let

$$E_{TOT} = \int_0^\infty [\mathscr{U}(k) + \mathscr{E}(k)]dk \tag{3.19}$$

be called the total energy. To the extent that the eddy viscosity contributes negligibly to the total energy dissipation, the overall energy balance is described by

$$2\lambda\ E_{TOT}=\int_0^\infty J(k)dk. \tag{3.20}$$

The streamfunctions are implicitly nondimensionalized by choosing the $J(k)$ to satisfy (3.20) with $\lambda=0.03$ and $E_{TOT}=1$. This value of λ was chosen to make the models correspond very roughly to the real atmosphere except of course that the forcing is isotropic and spread over a low wavenumber band of finite width.

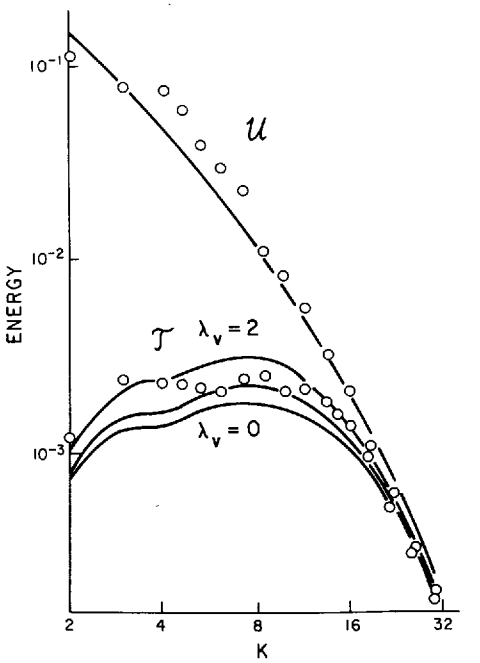

FIGURE 4 The barotropic energy spectrum $\mathcal{U}$, and the baroclinic kinetic energy spectrum $\mathcal{T}$, for the equilibrium solution of the closure equations (solid lines) and the equations of motion (discrete values).

The two sets of equations were stepped to approximate statistical equilibrium. Figure 4 compares the simulation and closure theory for three values of λ_v. The tendency to barotropy is so strong that the equilibrium large-scale flow is nearly barotropic despite the fact that the forcing is wholly baroclinic. The disagreement between the barotropic energy curves in Figure 4 is a remnant of the initial conditions in the simulation. The baroclinic curves

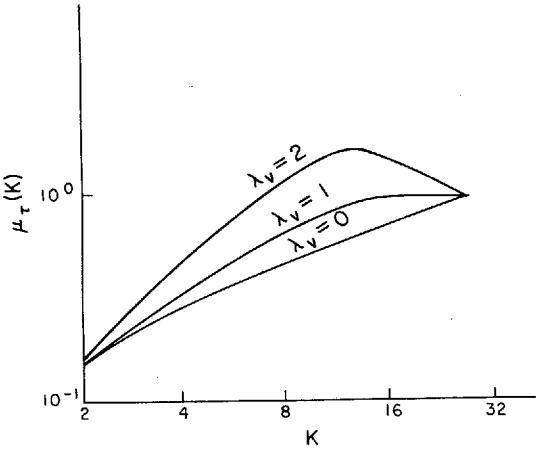

FIGURE 5 The baroclinic scrambling rate as a function of λ_v.

have ceased to change and most of the simulation points lie between the theoretical curves $\lambda_v=1$ and $\lambda_v=2$. It appears that the vortex stretching correction to $\mu_\tau(k)$ improves the agreement of the two solutions even for this low level of equilibrium baroclinicity. Figure 5 gives the curves for the $\mu_\tau(k)$ in each of the cases of Figure 4. The $\mu_\psi(k)$ change very little with λ_v and in all cases the curves for $\mu_\psi(k)$ differ insignificantly from that for $\mu_\tau(k)$ with $\lambda_v=0$. In the experiments described in the next section I have used $\lambda_v=1.5$ throughout.

4. EXPERIMENTS

In three experiments, I stepped the EDM closure equations (3.2–3.5, 3.7–3.11) to approximate equilibrium with a baroclinic forcing, vertical-boundary friction and eddy viscosity as in (3.17–3.18). In each experiment the wavenumbers run from $k_{\min}=1$ to $k_{\max}=128$ with $k_R=25$. For the forcing I let

$$J(k)=\begin{cases}\gamma k^{-1}, & k<k_F=3.25,\\ 0, & k\geqq k_F,\end{cases}$$

in (3.18) where γ is an adjustable constant. The three experiments differ only in the prescribed values for γ and λ, the boundary friction parameter. Let γ^* be the value of γ which satisfies the energy balance equation (3.20) between forcing and dissipation with $\lambda=0.03$ and total energy $E_{TOT}=1$. Table I gives the values of λ, γ and the equilibrium energies for each experiment. All

TABLE I
Summary of numerical experiments

Experiment	λ	γ	Energy Input Rate	Total Energy	Kinetic/ Available Potential	Rms Velocity (either layer)
A	0.03	γ^*	0.06	0.95	0.73/0.22	6.04 cm sec^{-1}
B	0.15	$5\gamma^*$	0.3	0.99	0.15/0.84	2.77 cm sec^{-1}
C	0.03	$5\gamma^*$	0.3	4.60	3.97/0.63	14.1 cm sec^{-1}

quantities are dimensionless unless the units are explicitly given. In all three experiments the eddy viscosity parameters have the values $\nu_0 = 0.0005$ and $k_e = 64$, and the eddy viscosity is counted as dissipation.

Although the dimensionless units are convenient, one naturally wants to interpret the results in a geophysical framework. With the ocean in mind, suppose k_R^{-1} corresponds to 40 km. Then the largest wavelength contained by the model is 6280 km and the high wavenumber cutoff corresponds to a "grid-point separation" of 25 km. With velocity scaled such that the rms velocity in either layer is as given in the last column of Table I, the boundary friction coefficient $\lambda = 0.03$ corresponds to dimensional $\lambda^{-1} = 387$ days. This value is consistent with the energy balance (3.20) for, say, an energy density of 25×10^6 ergs cm^{-2} and a production rate of 1.5 ergs cm^{-2} sec^{-1}. Experiment A corresponds to this choice. Experiments B and C were performed to test the sensitivity of the results to changes in the forcing and dissipation. In experiment B both the forcing and the friction parameter were increased by a factor 5 so that the total energy remains near unity. Experiment C has the forcing of B and the friction of A so that the total energy is near 5. In experiments A and B the equilibrium energy is less than unity by an amount which is equal to the fraction of the total energy dissipated by eddy viscosity.

Figure 6 shows the equilibrium energy spectra for each of the three experiments. In experiment A, as in the experiment of the previous section, most of the energy is in barotropic flow even though the forcing is wholly baroclinic. In experiment B, however, the equilibrium energy is largely baroclinic and the velocity fields in the two layers are negatively correlated in the forcing wavenumbers ($k < k_F$). At higher wavenumbers the flow is nearly barotropic, much as in experiment A. The total kinetic energy spectrum $\mathscr{U}(k) + \mathscr{T}(k)$, which would be measured by a current meter array in either layer, has its maximum at $k_{\min}$ in experiment A and near $k = 8$ in experiment B. Experiment C is qualitatively similar to A except that more barotropic energy reaches $k_{\min}$, where it "condenses" into a thin tower. In experiment C the lowest barotropic wavenumbers showed a slow but persistent adjustment up

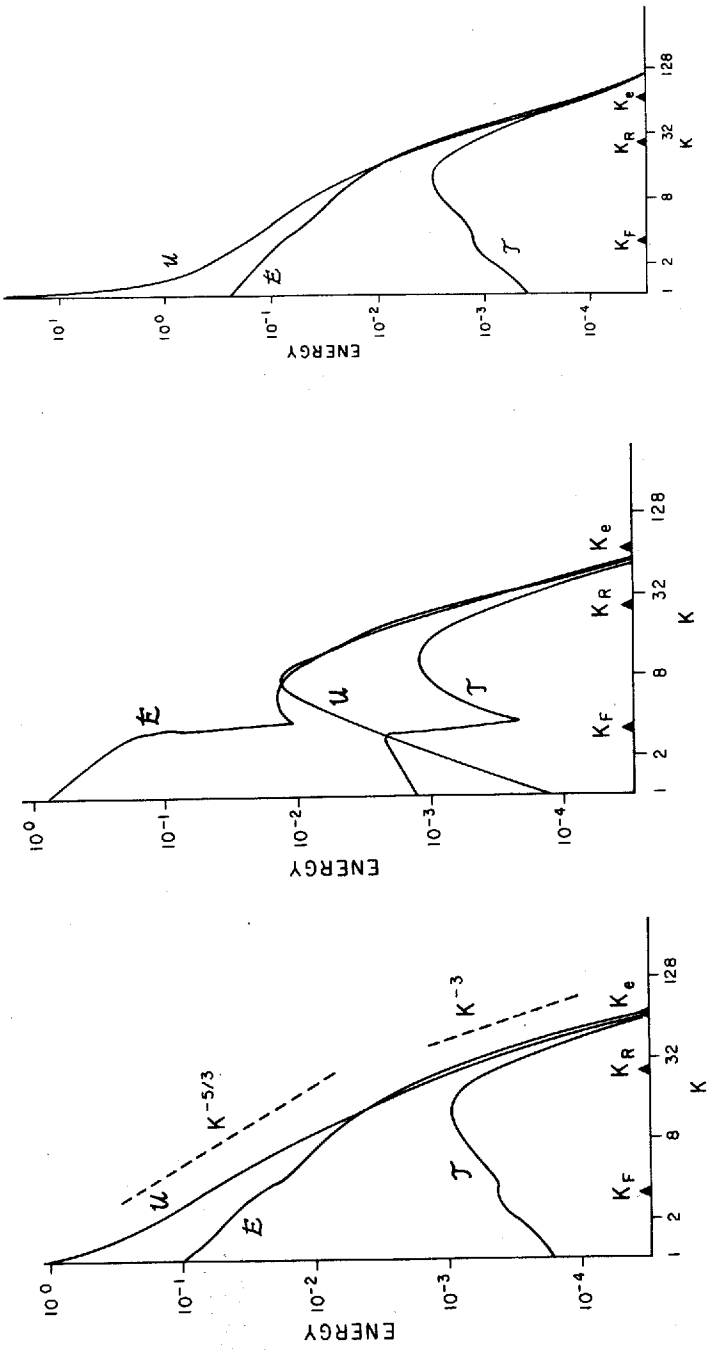

FIGURE 6 The equilibrium barotropic ($\mathcal{U}$), total baroclinic ($\mathcal{E}$) and baroclinic kinetic ($\mathcal{T}$) energy spectra for experiments A, B, and C.

to the time that the experiment was stopped, so that the system was not perfectly in equilibrium.

Experiments A and B differ most in the amount of equilibrium barotropic energy at low wavenumbers. The difference is primarily caused by the higher friction in B. In simple language, the leftward transfer of barotropic energy occurs so slowly that the stronger damping takes a heavy toll and much less energy reaches $k_{\min}$. This is especially well shown by Figure 7, which gives the energy transfer rates in the two types of triads. In Figure 7, $P(k)$ is the total rightward energy transfer past wavenumber k that occurs in UUU triads, and $Q(k)$ is the rightward transfer in UEE triads. The transfer rates are calculated from (3.2) in an obvious manner. Dashed lines represent negative values. As anticipated in Section 2, $P(k)$ is negative on $k < k_R$. $Q(k)$ reaches its maximum at k_F, the highest forced wavenumber, and falls off rapidly toward k_R as more and more of the energy enters the barotropic mode and begins to move leftward. Negative $P(k)$ drops sharply toward $k_{\min}$ in Figure 7b because of the large damping coefficient. The curves for experiment C are similar to Figure 7a except that $P(k)$ remains high down to $k_{\min}$.

Figure 8 shows the conversion of total baroclinic energy to barotropic energy in wavenumber k, defined by

$$C(k) = \iint^{\Delta} dp\, dq\, S(k, p, q),$$

where $S(k, p, q)$ is given by (3.3b). The quantity,

$$C_{\mathrm{TOT}} = \int_{k_{\min}}^{k_{\max}} C(k)\, dk,$$

is the "vertical-wavenumber" analog of $Q(k)$. In Figure 8 the value of $C(k)$ for experiment C has been divided by 5 to bring all three curves to a comparable scale. With this adjustment, the curves for experiments A and C are similar, but $C(k)$ for experiment B is much more strongly peaked. The difference between $C(k)$ in experiments A and B is consistent with the idea that the interactions comprising $Q(k)$ are more nonlocal in experiment B and therefore more like those of the baroclinic instability problem.

The energy transrer rates $P(k)$ and $Q(k)$ may be further subdivided into contributions from the six triad classes shown schematically in Figure 9. The top triangle in Figure 9 represents a barotropic triad in which two of the three members have wavenumbers less than k, while the second triangle represents a triad with two members greater than k. Only the triad classes sketched in Figure 9 can transport energy past k. Baroclinic instability falls into class $Q_4(k)$, but both $Q_1(k)$ and $Q_3(k)$ include "nearly isosceles" interactions of the same type. Class $Q_2(k)$ is unlike either baroclinic instability or two-dimensional turbulence.

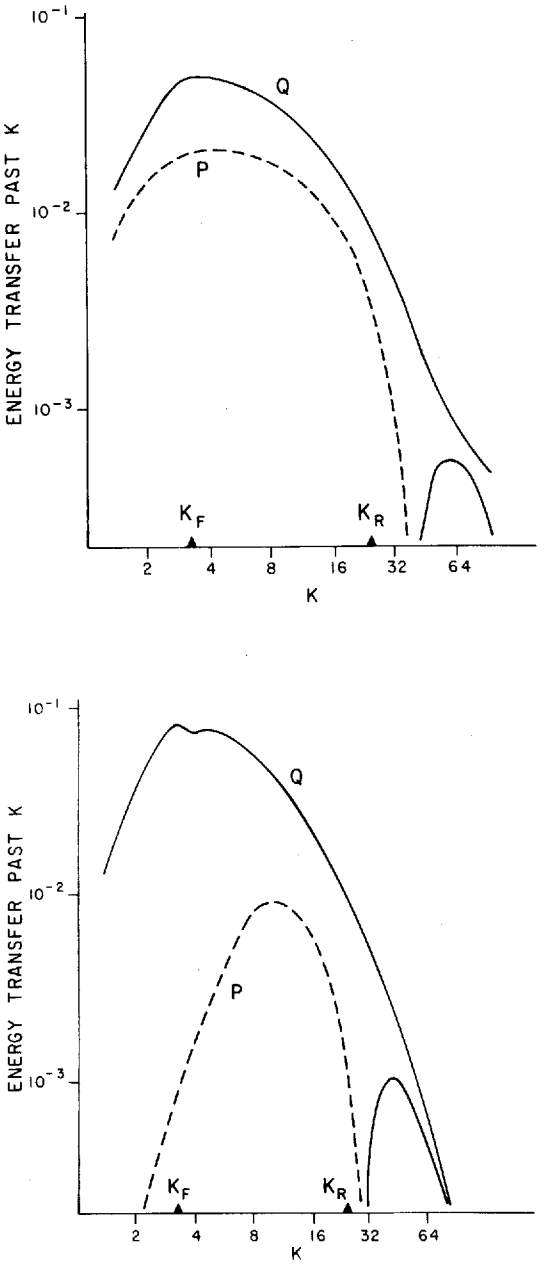

FIGURE 7 The rightward energy transfer past wavenumber k in UUU triads (P) and in UEE triads (Q) in (a) experiment A; and (b) experiment B. Dashed lines denote negative values.

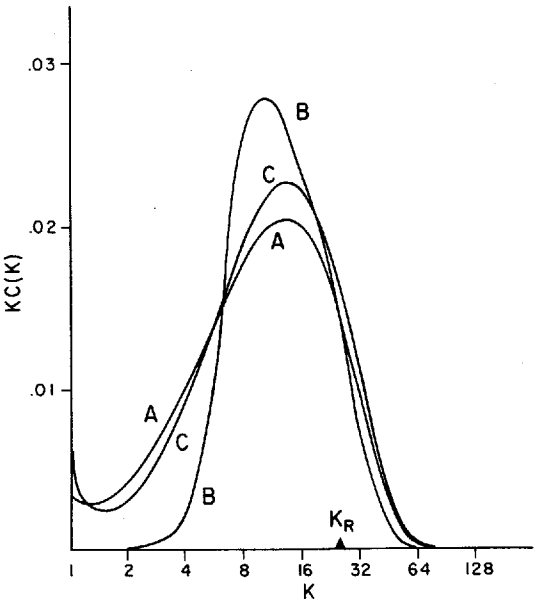

FIGURE 8 The conversion of total baroclinic energy into barotropic energy in wavenumber k in experiments A, B and C. The values for experiment C have been divided by 5.

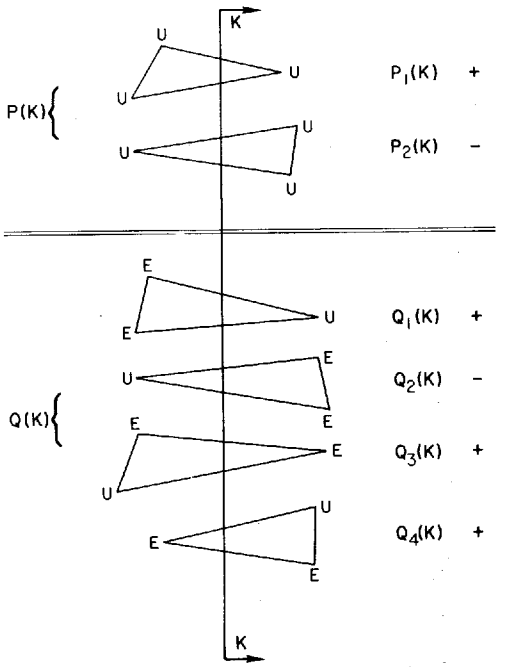

FIGURE 9 Triad classes that contribute to $P(k)$ and $Q(k)$. The arithmetical signs on the right are the expected signs of the contribution on $k < k_R$.

On the basis of general statistical mechanical principles, Kraichnan (1967) suggested that the average energy transfer is from the middle to the extreme wavenumbers in the triads of two-dimensional turbulence. The same logic applies to the two-layer system if $(k^2+k_R^2)^{1/2}$ replaces k in the ranking of baroclinic components. If all triad members have wavenumbers less than k_R, then Kraichnan's reasoning predicts that the contributions of the various classes to $P(k)$ and $Q(k)$ have the signs given on the right side of Figure 9. Figures 10 and 11, which are calculated from experiments A and B, support these qualitative predictions and show interesting quantitative differences between the two experiments. In experiment B, $Q_4(k)$ accounts for most of the rightward energy transfer, while the same transfer is about evenly divided between $Q_3(k)$ and $Q_4(k)$ in experiment A. This is further indirect evidence for a more nonlocal transfer in experiment B. The reverse transfer $Q_2(k)$ is significant in experiment A, but much less so in B.

Figure 12 gives an explicit measure of UEE triad nonlocalness. The quantity graphed is the fraction of

$$Q_1(k)+Q_3(k)+Q_4(k)$$

(all terms positive) which is accounted for by triads with at least one baroclinic member $E(p)$ in the forcing range, that is, with $p<k_F$. Again experiments A and C are similar, but B shows a much higher degree of nonlocalness.

5. DISCUSSION

My many simplifying assumptions probably destroy the possibility of useful direct comparison between geophysical observations and the experiments of the previous section. Both the atmosphere and ocean are distinctly inhomogeneous on large scales, and the equivalent layers assumption is especially bad for the ocean, where typical layer depths stand in the ratio 1:7 and the forcing is entirely in the upper layer. In both fluids, bottom topography and the latitudinal variation in the earth's effective rotation rate—the so-called "β-effect"—are also likely to be important.

Rhines (1975) and Holloway (1976) have studied the β-effect on two-dimensional turbulence. The varying rotation rate is a source for anisotropy and it supports linear Rossby waves which inhibit nonresonant triad interactions. The inhibition slows leftward energy transfer at low wavenumbers where the β-effect is the strongest. In the two-layer system, UEE triads also feel the β-effect, and stability theorists are already familar with the result that β stabilizes the very long waves in the baroclinic instability calculation.

Perhaps the most interesting result of the present study is the apparent sensitivity of the flow at low wavenumbers to changes in the friction. This is the

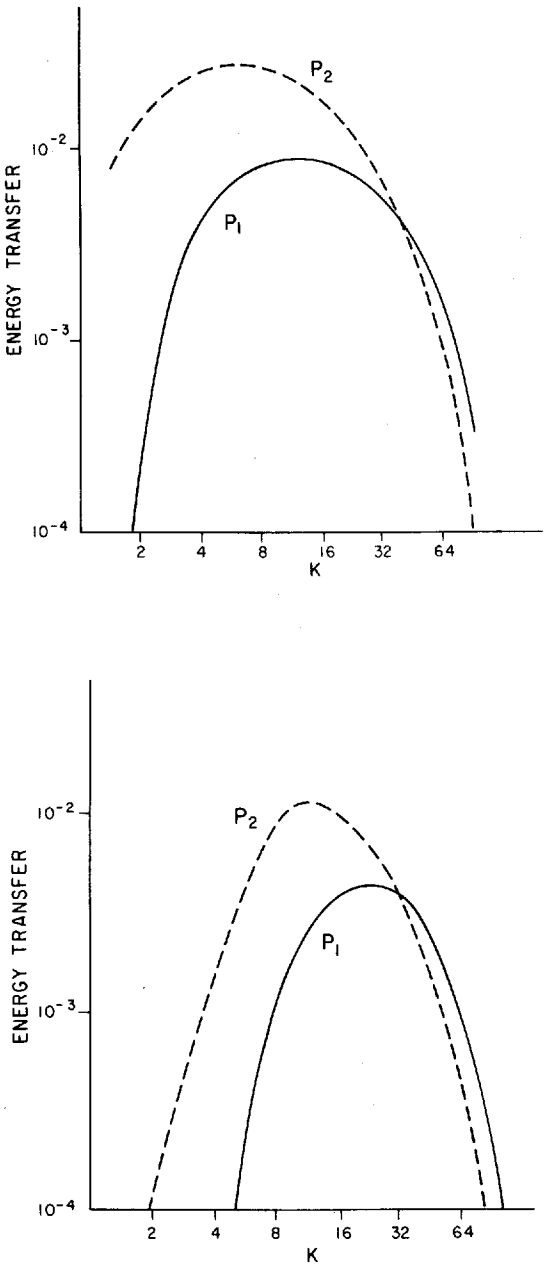

FIGURE 10 The contributions of $P_1(k)$ and $P_2(k)$ to $P(k)$ in (a) experiment A; and (b) experiment B. Dashed lines denote a negative contribution.

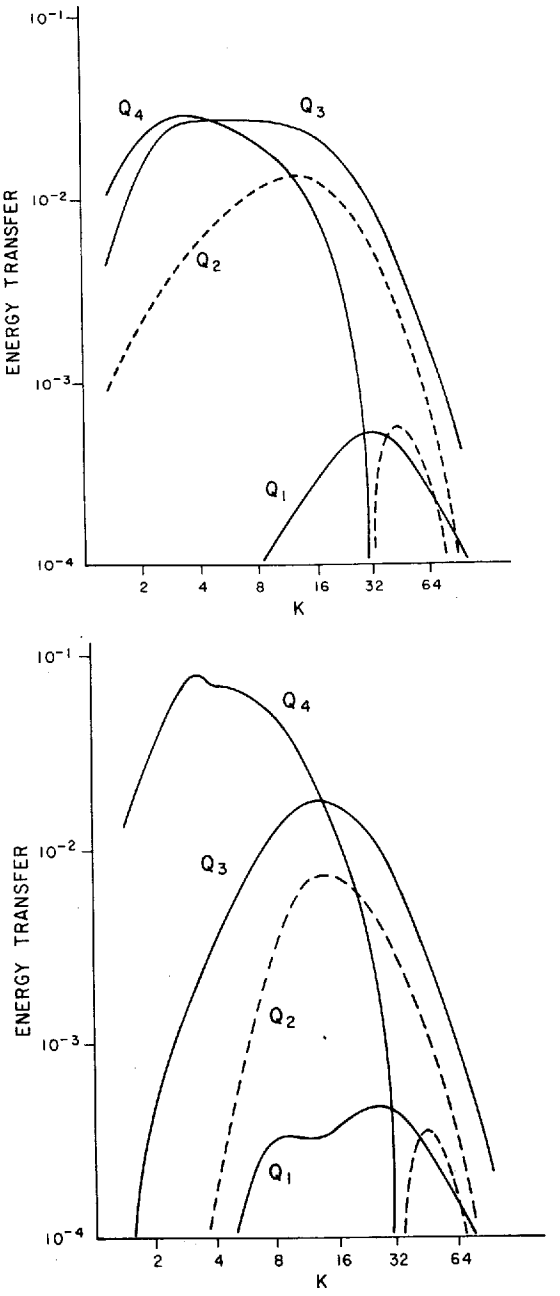

FIGURE 11 The contributions of $Q_1(k)$ through $Q_4(k)$ to $Q(k)$ in (a) experiment A; and (b) experiment B.

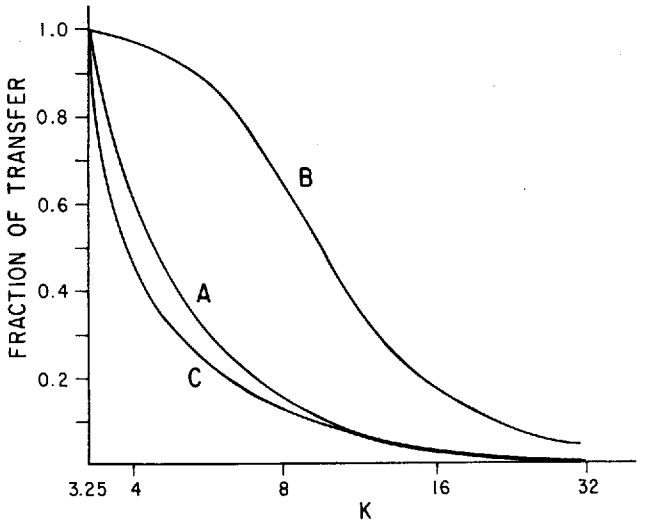

FIGURE 12 The fraction of the transfer $Q_1(k)+Q_3(k)+Q_4(k)$ past k which is accounted for by triads with at least one baroclinic component in the forcing range.

more interesting because ocean bottom topography and the β-effect also affect energy transfer and these combined factors vary significantly from place to place in the ocean. I suggest that the local mechanical energy budget in the ocean might be reasonably well characterized by cross-correlating year-long current meter records from different depths on the same mooring. If this is true, then a resource-efficient program for mapping mid-ocean dynamics might consist of widely separated single moorings placed at sites chosen for their different topographies and distances from coastal boundary currents.

Acknowledgments

I am indebted to Drs. Jack Herring and Greg Holloway of the National Center for Atmospheric Research for their help and advice. I am supported by the National Science Foundation (IDOE) as a part of the POLYMODE project.

Appendix

Let

$$B(a, b, c, d, e, f) = 4(e-f)\ (d-f)b^2c^2\ \sin(b, c)/(\text{def}),$$

where $\sin(b,c)$ is the sine of the interior angle opposite a in a triangle with sides of length a, b, c.

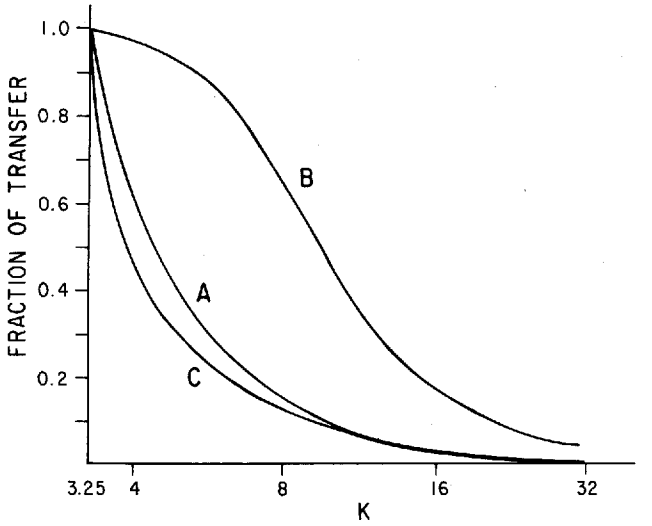

FIGURE 12 The fraction of the transfer $Q_1(k)+Q_3(k)+Q_4(k)$ past k which is accounted for by triads with at least one baroclinic component in the forcing range.

more interesting because ocean bottom topography and the β-effect also affect energy transfer and these combined factors vary significantly from place to place in the ocean. I suggest that the local mechanical energy budget in the ocean might be reasonably well characterized by cross-correlating year-long current meter records from different depths on the same mooring. If this is true, then a resource-efficient program for mapping mid-ocean dynamics might consist of widely separated single moorings placed at sites chosen for their different topographies and distances from coastal boundary currents.

Acknowledgments

I am indebted to Drs. Jack Herring and Greg Holloway of the National Center for Atmospheric Research for their help and advice. I am supported by the National Science Foundation (IDOE) as a part of the POLYMODE project.

Appendix

Let

$$B(a, b, c, d, e, f)=4(e-f)\ (d-f)b^2c^2\ \sin(b, c)/(\text{def}),$$

where $\sin(b,c)$ is the sine of the interior angle opposite a in a triangle with sides of length a, b, c.

Then

$$B_1(k, p, q) = B(k, p, q, k^2, p^2, q^2),$$

$$B_2(k, p, q) = B(k, p, q, k^2, p^2 + k_R^2, q^2 + k_R^2),$$

$$B_3(k, p, q) = -B(k, p, q, k^2 + k_R^2, q^2 + k_R^2, p^2),$$

$$B_4(k, p, q) = -B(k, p, q, \ , k^2 + k_R^2, p^2, q^2 + k_R^2),$$

$$B_5(k, p, q) = -B_3(k, p, q) - B_4(k, p, q).$$

References

Charney, J. G., "Dynamics of long waves in a baroclinic westerly current," *J. Meteor.* **4,** 135 (1947).

Charney, J. G., "Geostrophic turbulence," *J. Atmos. Sci.* **28,** 1087 (1971).

Eady, E. J., "Long waves and cyclone waves," *Tellus* **1,** 33 (1949).

Fjortoft, R., "On the changes in the spectral distribution of kinetic energy for two-dimensional non-divergent flow," *Tellus* **5,** 225 (1953).

Herring, J. R., Orszag, S. A., Kraichnan, R. H. and Fox, D. G., "Decay of two-dimensional homogeneous turbulence," *J. Fluid Mech.* **66,** 417 (1974).

Herring, J. R., "On the statistical theory of two-dimensional topographic turbulence," in press (1977).

Holloway, G., "Statistical hydromechanics: applications in mesoscale ocean circulation," Ph.D. thesis, University of California, San Diego (1976).

Holloway, G., "Stochastic closure for nonlinear Rossby waves," *J. Fluid Mech.* **82,** 747 (1977).

Holloway, G., "A statistical theory of nonlinear barotropic motion above irregular topography," in press (1977).

Kraichnan, R. H., "The structure of isotropic turbulence at very high Reynolds number," *J. Fluid Mech.* **5,** 497 (1959).

Kraichnan, R. H., "Lagrangian-history closure approximation for turbulence," *Phys. Fluids* **8,** 575 (1965).

Kraichnan, R. H., "Inertial ranges in two-dimensional turbulence," *Phys. Fluids* **10,** 1417 (1967).

Kraichnan, R. H., "An almost-Markovian Galilean-invariant turbulence model," *J. Fluid Mech.* **47,** 513 (1971a).

Kraichnan, R. H., "Inertial range transfer in two- and three-dimensional turbulence," *J. Fluid Mech.* **47,** 525 (1971b).

Kraichnan, R. H., "Eddy viscosity in two and three dimensions," *J. Atmos. Sci.* **33,** 1521 (1976).

Leith, C. E., "Atmospheric predictability and two-dimensional turbulence," *J. Atmos. Sci.* **28,** 145 (1971).

Leith, C. E. and Kraichnan, R. H., "Predictability of turbulent flows," *J. Atmos. Sci.* **29,** 1041 (1972).

Onsager, L., "Statistical hydromechanics," *Nuovo Cim. Suppl.*. 9, **6,** 279 (1949).

Orszag, S. A., "Numerical simulation of incompressible flows within simple boundaries. 1. Galerkin (spectral) representations," *Stud. Appl. Math.* **50,** 293 (1971).

Orszag, S. A., "Analytical theories of turbulence," *J. Fluid Mech.* **41,** 363 (1970).

Orszag, S. A., *Statistical Theory of Turbulence: Les Houches Summer School on Physics*, Gordon and Breach (1974).

Pedlosky, J., "Finite amplitude baroclinic waves," *J. Atmos. Sci.* **27,** 15 (1970).

Pedlosky, J., "Limit cycles and unstable baroclinic waves," *J. Atmos. Sci.* **29,** 53 (1972).

Pouquet, A., Lesieur, M., Andre, J. C. and Basdevant, C., "Evolution of high Reynolds number two-dimensional turbulence," *J. Fluid Mech.* **72,** 305 (1975).

Rhines, P. B., "Waves and turbulence on a beta-plane," *J. Fluid Mech.* **69,** 417 (1975).

Rhines, P. B., "The dynamics of unsteady currents," in *The Sea* Vol. VI, John Wiley and Sons, New York (1977).

Salmon, R., Holloway, G. and Hendershott, M. C., "The equilibrium statistical mechanics of simple quasi-geostrophic models," *J. Fluid Mech.* **75,** 691 (1976).